Perfluoroalkyl End-Functionalized Oligoesters: Correlation between Wettability and End-Group Segregation

Alla Synytska,*,† Dietmar Appelhans,† Zhong Gang Wang,§ Frank Simon,† Frank Lehmann,‡ Manfred Stamm,† and Karina Grundke†

Leibniz Institute of Polymer Research Dresden, Hohe Str. 6, D-01069 Dresden, Germany; Synthopol Chemie Dr. rer. pol. Koch GmbH & Co. KG, Alter Postweg 35, D-21614 Buxtehude, Germany; and Department of Polymer Science and Materials, Dalian University of Technology, Zhongshan Road 158 116012 Dalian, Republic of China

Received May 21, 2006; Revised Manuscript Received November 17, 2006

ABSTRACT: We report a detailed investigation of the processes of the surface segregation in correlation with the wetting properties of perfluoroalkyl end-functionalized linear aromatic oligoesters. We have compared properties of films containing different fluorine concentration prepared by the spin-coating technique and by melting of polymer grain onto the supported substrate. We demonstrate that both methods can be used for the preparation of highly hydrophobic and oleophobic surfaces. Obtained layers possess high value of *n*-hexadecane advancing contact angle and low contact angle hysteresis. Moreover, oligoester films with the surface energies as low as 11 mJ/m^2 were prepared with 10.7 wt % of fluorine in the system and possessed higher oleophobicity than Teflon AF. We showed that the advantages of use of melting of polymer grain are higher surface enrichment and closer packing of perfluorinated species and, as a result, a higher hydro/oleophobicity, especially at lower F contents (<6 wt %). This is a first report about an influence of preparation method onto the surface properties of perfluorinated polymers.

Introduction

The design of versatile fluorinated polymer materials is a challenging task for modern coating industry, microelectronics, and biomedical applications.[1,2] Incorporation of fluorine atoms to a polymer renders its surface free energy substantially lower. This leads to a low wettability toward high and moderate polar liquids and usually to weak adhesion joins. Desired fluorinated polymers architectures can be hardly obtained by common polymerization techniques. Different methods, including blending,[3,4] copolymerisation,[5−8] chemical surface reactions,[9] and flame and plasma treatment,[10,11] have been successfully applied for the preparation of partly fluorinated polysiloxanes,[12] poly(acrylates),[13] polymethacrylates,[14,15] and polystyrenes.[16−18]

In general, fluorinated polymers can be divided into several classes depending on the position of fluorine groups in the polymer chains. The fluorine moieties can be a part of either polymer backbone, side, or terminating groups. It was shown that the surface activity of fluorine moieties can be enhanced considerably in polymers with a fluorinated terminating group. Low surface free energy due to the strong surface segregation of the fluorinated moieties is the result.[18−25]

Uniformly end-functionalized polymers have been applied to be useful model systems for studying surface segregation. Using perfluoroalkyl-terminated polymers,[19] it was experimentally shown that the perfluorinated segments tend to segregate in the surface region and enhance the surface concentration of fluorine up to 7.6 times compared with its bulk concentration. Chen et al.[25] showed that hydrophobic end groups are preferentially concentrated at the air interface while the hydrophilic end groups remain in the bulk. Affrossman et al.[26] reported results for styrene polymers, having one or both ends capped with perfluorinated groups. They show preferential surface migration of the low-energy end groups that scales with their bulk concentration. Hirao et al.[24] reported an influence of the number of chain-end and in-chain perfluorooctyl groups on the processes of surface segregation. He showed that the degree of the surface enrichment increased with the number of perfluorooctyl groups and, on the other hand, decreased with increasing molecular weight of the functionalized polymer. Moreover, the terminal group was found to be more effective for the surface enrichment than the internal one. This indicates that the terminal group is more mobile than the internal fluorinated segment.[16−18,27] On the basis of theoretical and experimental considerations, Koberstein et al.[18] showed that the location of low-energy functional groups at one chain end is decisive for design of liquid-repellent coatings.

The most of investigations report perfluorinated oligo- and polyesters with aliphatic main chain, and only few investigations can be found about aromatic ones.[26] However, aromatic polyesters have distinct advantages and are used in the coating industry to provide good resistance to mineral oils, solvents, and acids. Incorporating fluorinated groups in such materials can enhance these properties and other desired properties, such as water repellence of the coating. To the best of our knowledge, in most studies polymer surface properties were investigated on model systems prepared from spin-coated films. In part, spin-coated films lead very often to dewetting processes. Namely, thick melt layers are more relevant for industrial coating applications.

Thereby, the aim of this work was a systematic investigation of the influence of conditions of preparation onto processes of fluorine surface segregation and surface properties of linear aromatic perfluoroalkyl functionalized oligoesters. We have compared the fluorine segregation in thin films (thickness 100 nm) prepared by spin-coating and subsequent annealing and by

* Corresponding author. E-mail: synytska@ipfdd.de.
† Leibniz Institute of Polymer Research Dresden.
‡ Synthopol Chemie Dr. rer. pol. Koch GmbH & Co. KG.
§ Dalian University of Technology.

10.1021/ma061139i CCC: $37.00
Published on Web 12/23/2006

Scheme 1. Schematic of the Synthesis of Linear Aromatic End-Group-Functionalized Oligoesters (A) and Teflon AF (B)

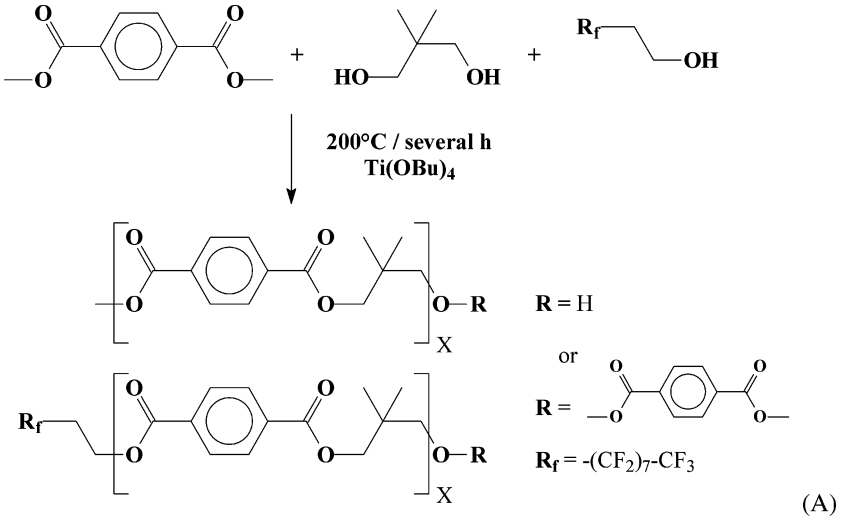

melting of polymer grain onto the supported substrate (film thickness 10 up to 15 μm) at different concentration of perfluorinated groups. We have also investigated the possibilities to design water and oil-repellent surfaces based on melt and spin-coated films from perfluoroalkyl end-functionalized linear aromatic oligoesters. We have deeply analyzed wettability of prepared surfaces in context of advancing, receding contact angles, and contact angle hysteresis. Hydro/oleophobicity of investigated aromatic oligoesters was also compared with commercially available fluorinated polymer Teflon AF.

This study has both fundamental and application aspects offering a step toward a deeper understanding of the correlations between the molecular surface composition of aromatic perfluoroalkyl-substituted polymers indented for design of real coatings and their macroscopic surface properties.

Experimental Part

Materials. Linear aromatic end-group-functionalized oligoesters were synthesized by melt polycondensation at 200 °C in vacuum, using $Ti(OBu)_4$ as catalyst (Scheme 1). Their main polymer chain has a linear structure consisting of a sequence of terephthalate and neopentylglycol alternating groups. The fluorinated oligoesters were modified with a $-C_8F_{17}$ perfluorinated tail attached to the main oligomer chain via ester bonds (Scheme 1). The molecular weight (M_w) of oligoesters was in the range of about 2000 and 2800 g/mol (PDI $\sim$ 1.7) (Scheme 1). The fluorine bulk content varies from %F = 0 wt % to %F = 10.72 wt %. According to DSC data, the glass transition temperature of all samples ranges from T = 14 to 30 °C (Table 1). All oligoesters are amorphous.

Film Preparation. Polished silicon wafers (100) with a native silicon oxide layer of a thickness of ca. 1.7 nm were purchased from Silchem Handelsgeselschaft GmbH (Freiberg, Germany) and Wacker-Chemicronics GmbH (Burghausen, Germany). Wafers were washed three times with dichloromethane in an ultrasonic bath for 5 min and afterward in a mixture of water, ammonia solution (25%), and hydrogen peroxide (30%) in volume ratio of 1:1:1 at 60 °C for 1 h. The substrates were rinsed 5−6 times in deionized reagent grade water and then dried with nitrogen flux.

A 2 wt % polymer solution in purified $CHCl_3$ (Sigma-Aldrich) was filtered through a porous PTFE filter (with pores of 0.25 μm in diameter). Thin polymer films were prepared by spin-coating (Headway) at 2000 rpm for 30 s. After spin-coating, the solvent was evaporated at room temperature for 24 h. Then, the samples were annealed in a vacuum oven at 20 °C above T_g for 24 h. Melt films were prepared by melting of polymer grain on the supported substrate (spin-coated layer from the same polymer) for 1 h at 180 °C in a vacuum oven.

Table 1. Characteristics of Used Oligoesters: Bulk Fluorine Content (%F^{bulk}), Glass Transition Temperature (T_g), Averaged Number (M_n) and Weight (M_w) Molecular Weights, and Polydispersity (PDI)

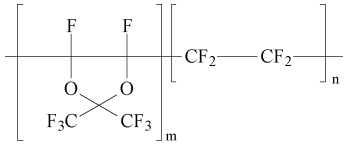

m : n = 65 : 35 (B)

sample ID	%F^{bulk} (wt %)	T_g (°C)	M_n (g/mol)	M_w (g/mol)	PDI
LO-F_8#1	0.00	14	1300	2600	1.69
LO-F_8#2	2.54	19.2	1400	2800	2.00
LO-F_8#3	3.25	23	1500	2600	1.73
LO-F_8#4	6.24	30	1200	2000	1.67
LO-F_8#5	10.72	25	1300	2200	1.69

Film Characterization. The thickness of spin-coated oligoester films was measured by a Multiscope Optrel (Berlin, Germany) null ellipsometer. Initially, the thickness of the native SiO_2 layer (usually 1.7 ± 0.2 nm) was calculated at refractive indices N = 3.858-i0.018 for the Si substrate and n = 1.4598 for the SiO_2 layer. The thickness of polyester layers was evaluated applying the three-layer model Si/SiO_2/oligoester using the measured value n = 1.7 for the refractive index of oligoesters. The thickness of the spin-coated oligoester layers was measured to be on the order of 100 nm. The thickness of the melt layers was measured using a scratch test. In this case, an optical imaging device (MicroGlider, Bergish Gladbach, Germany) and scanning force microscopy, SFM (DI III, Digital Instruments) were applied. The thickness of melt layers ranged from 10 to 15 μm.

The surface topography was examined using the scanning force microscope (SFM, DI III, Digital Instruments) and the optical imaging device (MicroGlider, Bergish Gladbach, Germany). In SFM measurements the tapping and phase modes were used to map the film morphology at ambient conditions. Silicon tips with a spring constant of 1.5−6.3 N/m and a resonance frequency of 63−100 kHz were used. The roughness characteristics were obtained from 20 × 20 μm^2 (SFM) and 1 × 1 mm^2 (MicroGlider) large images. The resolution of each SFM and MicroGlider image taken was 512 × 512 and 1000 × 1000 lines, respectively.

The root-mean-square (rms) roughness was calculated from SFM and MicroGlider images with the Nanoscope III and Mark III software, respectively. The roughness factor, r_s,[28] which is a ratio between the real (true, actual) surface area and the geometric surface area, was calculated from SFM images and was found to be 1.004−1.008 for all systems (Table 2). The rms roughness obtained from

Table 2. Roughness Parameters for Spin-Coated (s) and Melt (m) Films Obtained from MicroGlider and SFM Measurements

		rms roughness (nm)					
		microGlider (1 mm × 1 mm)		SFM (20 μm × 20 μm)		roughness factor r_s (SFM)	
sample ID	$\%F^{bulk}$ (wt %)	s	m	s	m	s	m
LO-F_8#1	0.00	10	11	<1	<1	1.004	1.004
LO-F_8#2	2.54	11	12	<2	<2	1.006	1.005
LO-F_8#3	3.25	10	11	<2	<2	1.008	1.008
LO-F_8#4	6.24	12	12	6	8	1.007	1.008
LO-F_8#5	10.72	15	15	10	12	1.005	1.006

the MicroGlider data is in the range from 10 to 15 nm for all systems. The SFM data revealed that the rms roughness values are in the order of several nanometers (Table 2).

It should be noted that there is a tendency toward higher values of rms roughness for samples with the higher bulk fluorine content (Table 2). Nevertheless, all roughness values are in a range where no significant influence on the wettability is expected.

Advancing and receding contact angles were measured by the sessile drop method using axisymmetric drop shape analysis (ADSA) and a conventional drop shape technique (Krüss DSA 10, Hamburg, Germany). The ADSA technique was applied to measure the contact angle of liquids on the spin-coated films. Details of the procedure and the experimental setup for low-rate dynamic contact angle measurements by ADSA are given elsewhere.[29] In this work, at least five dynamic water contact-angle measurements at velocities of about 0.2 mm/min were performed. Low-rate dynamic contact angles at these velocities are essentially identical with the advancing contact angles obtained by the conventional drop shape technique.[30] The latter technique was used to determine advancing and receding liquid contact angles for melt films. At least five separate measurements for each of five samples were used to calculate a mean contact angle. The standard deviation did not exceed 2°−3° for advancing and receding contact angles, respectively. All contact angle measurements were carried out at 24 ± 0.5 °C and relative humidity of 40 ± 3%, which were kept constant.

The advancing contact angles were used to calculate the solid surface tension γ_{sv} using the equation-of-state approach (EQS):[31,32]

$$1 + \cos\theta_e = 2\sqrt{\frac{\gamma_{sv}}{\gamma_{lv}}}\, e^{-\beta(\gamma_{lv}-\gamma_{sv})^2} \qquad (1)$$

where β is an empirical parameter and was found to be 0.000 124 7 $(mN/m)^{-2}$, γ_{sv} and γ_{lv} denote the interfacial tensions of the solid−vapor and liquid−vapor interfaces, respectively, and θ_Y is the Young contact angle.

High purity deionized water (W) (γ_{lv} = 72.0 mN/m) and *n*-hexadecane (HD) (γ_{lv} = 27.5 mN/m) were chosen as model liquids to investigate the wettability of oligoester films. Contact angles of these liquids (water and *n*-hexadecane)[33] are accepted as indices of hydrophobicity and oleophobicity,[34] respectively.

It was shown by our group and by others[31,35−37] that the experimental contact angle patterns were obtained for a large number of polar and nonpolar liquids on different solid surfaces containing also polar groups in their surface region. Such pattern imply that the contact angle of a liquid drop on a certain solid surface appears to depend almost entirely on the liquid−vapor surface tension and very little on the other properties of the liquid. Therefore, eq 1 should be applicable for the evaluation of surface free energy from the contact angles obtained for both water and *n*-hexadecane.

Angle-resolved X-ray photoelectron spectroscopic measurements (ARXPS)[38] were carried out by means of an AXIS ULTRA photoelectron spectrometer (KRATOS ANALYTICAL, Manchester, England). The spectrometer was equipped with a monochromatic Al Kα ($h\nu$ = 1486.6 eV) X-ray source of 300 W at 15 kV. The kinetic energy of photoelectrons was determined with a hemispheric analyzer set to pass energy of 160 eV for wide-scan spectra and 20 eV for high-resolution spectra, respectively. During all measurements, electrostatic charging of the sample was avoided by means of a low-energy electron source working in combination with a magnetic immersion lens. Later, all recorded peaks were shifted by the same value that was necessary to set the C 1s peak to 284.70 eV. Quantitative elemental compositions were determined from peak areas using experimentally determined sensitivity factors and the spectrometer transmission function. Spectrum background was subtracted according to Shirley.[39] The high-resolved spectra were dissected by means of the spectra deconvolution software. Free parameters of component peaks were their binding energy (BE), height, full width at half-maximum, and the Gaussian−Lorentzian ratio.

XPS is a highly surface sensitive technique, where the information depth is not higher than 10 nm in maximum. Tilting the samples under the analyzer can enhance the surface sensitivity of the method. All polymer samples were measured at the three different takeoff angles Θ = 0°, 60°, and 75°. Here, the takeoff angle is defined as the angle between the surface normal and the electron-optic axis of the spectrometer. The corresponding information depths for the C 1s level are 10 nm (for Θ = 0), 5 nm (for Θ = 60°), and 2.5 nm (for Θ = 75°).

Results and Discussion

Previous studies revealed that migration and reorganization of fluorine moieties, which determine the solid surface free energy of polymer films, occur in the topmost layer of the surface with a thickness of about 1−2 nm.[21−24,40,41] Consequently, it can be assumed that the surface properties of thicker polymer films are independent of their thickness. Therefore, the difference between the surface properties of spin-coated and melt films is solely caused by the preparation conditions, i.e., conditions of annealing.

The values of advancing and receding contact angles of water (W) and *n*-hexadecane (HD) on spin-coated and melt oligoester films as a function of bulk fluorine content are presented in Figure 1.

It is obvious that the water advancing contact angle, θ_A^W, for spin-coated and melt films steadily increases with an increasing bulk fluorine content (%F) (Figure 1a). Very hydrophobic surface with the highest value of θ_A^W (θ_A^W = 120°) is obtained for the system with %F = 10.72 wt % (LO-F_8#5) and is independent of the film preparation conditions. It can be assumed that LO-F_8#5 possess preferentially organized CF_3 groups on the top of the surface.

However, the melt films possess a slightly higher hydrophobicity compared to the spin-coated ones when the bulk fluorine content ranges between %F = 2.54% and %F = 6.24 wt %. In this case, the values of advancing water contact angle on the melt films are higher than those on the spin-coated ones (Figure 1a). For example, the LO-F_8#4 surface demonstrates a slightly higher value of θ_A^W value for melt films (θ_A^W = 113°) comparing to that of spin-coated ones (θ_A^W = 110°). This difference in value of θ_A^Wcan be indication for a denser alignment of the R_f end chain in the melt films, meaning a higher content of CF_3 groups at the surface compared to the less annealed spin-coated films.

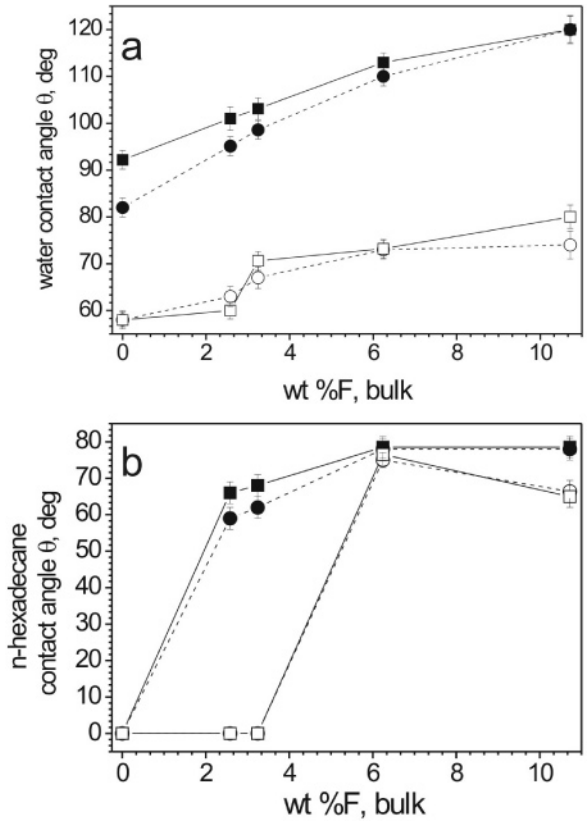

Figure 1. Mean advancing (solid symbols) and receding (open symbols) contact angles of water (a) and *n*-hexadecane (b) for the melt (■, □) and spin-coated (●, ○) films perfluorinated oligoesters vs bulk fluorine content.

Figure 1b summarizes the values of *n*-hexadecane (HD) advancing (θ_A^{HD}) and receding (θ_R^{HD}) contact angles on the oligoester surfaces at different bulk fluorine contents. We found that HD wets the surface of the nonfluorinated (%F = 0 wt %) oligoester completely. From the values of water advancing contact angles measured on nonfluorinated samples, the solid surface free energy of oligoesters was calculated to be γ_{sv} = 37.7 mJ/m^2 and γ_{sv} = 30.2 mJ/m^2 for the spin-coated and the melt film, respectively. These values are in reasonably good agreement with the literature values of the critical surface tension, γ_c, for nonfluorinated oligoesters, which typically ranges from γ_c = 32 to γ_c = 35 mN/m.[34,42,43] Therefore, it is not surprising that *n*-hexadecane, which has a lower surface tension of γ_{lv}= 27.5 mN/m, wets surface of nonfluorinated oligoesters completely (θ_A^{HD} and θ_R^{HD} of 0° were measured (Figure 1b)). The lower values of surface free energy for the melt films can be explained by the stronger enrichment of the topmost surface region with nonpolar alkyl groups and depletion with the oxygen-containing groups comparing to that of the spin-coated ones.

For the perfluorinated oligoesters with the lowest bulk fluorine content (%F = 2.54 wt %), advancing HD contact angles of θ_A^{HD} = 59° and θ_A^{HD} = 66° were measured on the spin-coated and melt films, respectively (Table 3). Apparently, incorporation of a small amount of fluorinated species (about 3 wt %) into the oligoester results in strong increase of *n*-hexadecane advancing contact angle. Similar to the case of water, the θ_A^{HD} increases with increasing bulk fluorine content. The values of θ_A^{HD} are even higher for the melt films comparing to the spin-coated ones. A higher concentration and closer packing of perfluorinated terminal groups in the topmost surface region may cause this fact.

Increase of fluorine concentration (%F = 6.24 and %F = 10.72 wt %) in the system results in further increase of the advancing *n*-hexadecane contact angle (Figure 1b). In this case, HD contact angles reached plateau values (about 80°) at higher fluorine concentrations (%F = 6.24 and %F = 10.72 wt %). It is well-known that not the value of advancing contact angle alone but in combination with the value of contact angle hysteresis (difference between advancing and receding contact angle) is a direct reflection of the surface wettability.[5,7,30,35] Here it is remarkable that the contact angle hysteresis for *n*-hexadecane is very small for these samples (%F = 6.24 and %F = 10.72 wt %) and is of about 2°−10°. In other words, these oligoesters possess oleophobic surface properties and repel oil droplets such as *n*-hexadecane. It should be noted that the advancing and receding HD contact angles for the oligoester surfaces with %F = 6.24 wt % ($\theta_A^{HD}/\theta_R^{HD}$ = 78.5°/76.5°) are higher than those measured in this work for the reference hydrophobic amorphous fluoropolymer Teflon AF ($\theta_A^{HD}/\theta_R^{HD}$ = 66°/65°) or given in our previous study.[37] This observation demonstrates a higher oleophobicity of the perfluorinated oligoesters compared to the Teflon AF. Most probably, such differences in HD contact angles for Teflon AF and LO-F8#4, LO-F8#5 films can be caused by different degree of alignment of the oligoester chains and more pronounced surface enrichment and alignment of $-CF_3$ groups on the top of the surface.

Regarding the hydrophobicity of the perfluorinated oligoester films, there are, in fact, very high values of the water advancing contact angles; θ_A^W are in the range of 110°−120°. On the other side, values of water receding angle of about $\theta_R^W \approx 70°$ were measured. Thereby, the water contact angle hysteresis, which is a difference between advancing and receding contact angles, is of about 40° (Figure 1a, Table 3). Now, the perfluorinated oligoester films appear less hydrophobic than some fluorinated polymers such as Teflon AF, which possess very high values of advancing and receding contact angles (of about 120°). Most probably, oxygen-containing polar groups are reoriented toward the outermost surface region when the films are in contact with highly polar liquids such as water resulting in relatively low values of water receding contact angle. Summing up the obtained values of contact angles of both liquids, we can conclude that the water advancing contact angles are sensitive to the presence of hydrophobic perfluorinated species and the receding contact angles are more sensitive to the more polar nonfluorinated species available in the surface region of the oligoester.

A solid surface free energy γ_{sv}, calculated from the advancing contact angle of water, is γ_{sv} = 11.4 mJ/m^2 for the surfaces with the highest bulk fluorine content (%F = 10.72 wt %). Using the EQS (eq 1, see Experimental Part), we predict the value of *n*-hexadecane contact angle to be 75°. This is in good agreement with the measured value of advancing HD contact angle, which is θ_A^{HD} = 78.5° for the system LO-F$_8$#4 (%F = 6.24 wt %, Table 3). From this value of HD contact angle, the γ_{sv} value of 10.7 mJ/m^2 is calculated. Such relatively low values of the solid surface free energy clearly indicate a significant enrichment of the topmost layer of the oligoester films with perfluorinated groups. Notably, that the calculated values of the solid surface free energy correspond to the surface which is mainly composed of highly aligned $-CF_3$ groups.[34,42]

However, there is a discrepancy between the values of the surface free energy calculated from the experimental values of water and *n*-hexadecane advancing contact angles for the films with bulk fluorine contents in the range from %F = 2.54 wt % to %F = 6.24 wt %. The calculated solid surface free energy

Table 3. Advancing Water (W) and *n*-Hexadecane (HD) Contact Angle Data and Fluorine Surface Atomic Concentration (Obtained from ARXPS Analysis) for Spin-Coated and Melt Oligoester Films[a]

		spin-coated films			melt films		
sample ID	$\%F^{bulk}$ content (%)	$F^{surface}$ content, (%)	CA_W^{ADV} (deg)	CA_{HD}^{ADV} (deg)	$F^{surface}$ content, (%)	CA_W^{ADV} (deg)	CA_{HD}^{ADV} (deg)
LO-F_8#1	0.00	0.00	82.0 ± 1.7	0.0	0.00	92.2 ± 2.0	0.0
LO-F_8#2	2.54	26.25	95.1 ± 1.5	59.0± 2.5	34.64	101.0 ± 1.8	66.0 ± 2.7
LO-F_8#3	3.25		98.6 ± 2.0	62.0± 2.3		103.1 ± 1.9	68.0 ± 2.7
LO-F_8#4	6.24	35.05	110.0 ± 1.6	78.5± 2.5	37.40	113.0 ± 2.0	78.5 ± 2.3
LO-F_8#5	10.72	36.19	120.0 ± 2.0	78.5± 2.5	39.20	120. ± 2.0	78.5± 2.6

[a] Fluorine surface content is calculated from ARXPS results obtained at 75° incidence angle (this corresponds to about 2 nm information depth).

from the values of HD contact angle range from $\gamma_{sv} = 16.3$ mJ/m^2 (%F = 2.54 wt %) to $\gamma_{sv} = 10.7$ mJ/m^2 (%F = 10.72 wt %), whereas the calculation based on the water contact angles results in values between $\gamma_{sv} = 25.8$ mJ/m^2 for the lowest (%F = 2.54 wt %) and $\gamma_{sv} = 11.4$ mJ/m^2 for the highest (%F = 10.72 wt %) bulk fluorine contents, respectively. One reason might be that water is a highly polar liquid and *n*-hexadecane is a nonpolar one. Therefore, *n*-hexadecane contact angles may be especially sensitive to the changes in the surface concentration of nonpolar perfluorinated tails although water contact angles are sensitive to the presence of both nonfluorinated and perfluorinated groups in the surface region.

In general, on the basis of contact angle results, we can assume the possibility to realize more densely packed perfluorinated end groups the top of the surface of melt films. We note that obtained results of the wettability of perfluorinated aromatic oligoesters are in a good agreement with the results obtained by other authors (see for example publication of Grampel et al.[21,23,41] for partially fluorinated polymethacrylates or fluorinated blocked isocyanates). However, in most reported cases authors consider the hydrophobicity of surfaces of perfluorinated polymers in the terms of advancing contact angle. However, values of both advancing and receding contact angles have to be considered to make a proper conclusion about "true" hydro/oleophobicity.[31,44] We emphasize that this report gives a thorough investigation of the hydro/oleophobicity of perfluorinated oligoesters and have been performed analyzing behavior of two liquids (polar and nonpolar) taking into account both advancing and receding contact angles.

For a proper interpretation of the wetting behavior it is important to have a direct evidence of the surface segregation of both perfluorinated and the oxygen-containing polar groups. Therefore, the chemical composition of the topmost surface region was quantitatively analyzed by ARXPS.

The depth profiles of the concentration of fluorine- and oxygen-containing moieties in the surface region are summarized in Figure 2. The value of the F:C ratio increases with a decrease of the information depth for both spin-coated and melt films (Figure 2a). However, melt layers demonstrate a stronger enrichment by perfluorinated species in the topmost region compared to the spin-coated ones (Figure 2a). To compare the results for the different perfluorinated oligoesters, the relative enrichment *Q* was calculated as the ratio of the surface fluorine concentration to the bulk one for each investigated system. The enrichment factor decreases with the increase of the bulk fluorine contents for both spin-coated and melt films (Table 4). This indicates that the effect of incorporation of small amount of the perfluorinated tails on the *Q* is reduced with increasing the bulk fluorine contents. In other words, the perfluorinated groups in the topmost surface layer hamper the migration of additional perfluorinated tails to the surface when the bulk fluorine content increases. The relative enrichment also decreases with increasing information depth, demonstrating that the fluorine moieties are

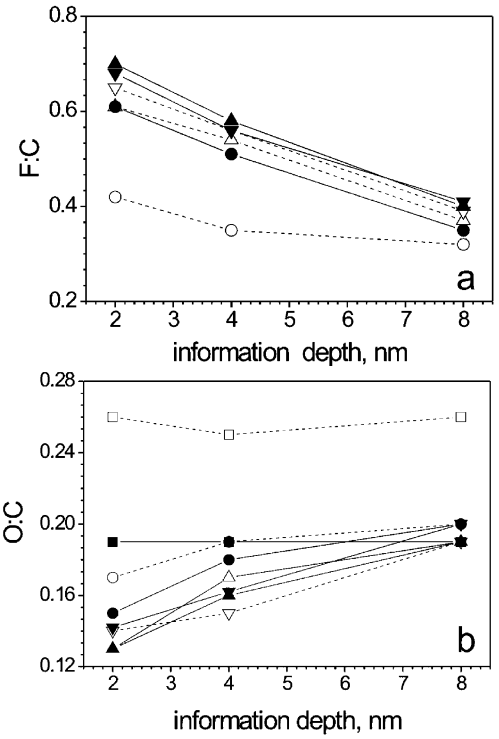

Figure 2. Depth profiles of the F:C (a) and O:C (b) ratio for spin-coated (open symbols) and melt (solid symbols) films with various bulk fluorine contents: (■, □) 0 wt %; (●, ○) 2.54 wt %; (▲, △) 6.24 wt %; (▼, ▽) 10.72 wt %.

concentrated on the surface. The higher value of *Q* is found for the melt films compared to the spin-coated ones. For example, in the topmost 2 nm layer of the melt film with %F = 2.54 wt % *Q* is equal to *Q* = 22.6, while for the spin-coated sample *Q* is found to be *Q* = 15.6 (Table 4).

On the other hand, the O:C atomic ratio, indicating the polar functional groups of the oligoester, decreases with a decrease of the information depth. This designates a reduced amount of ester groups in the topmost layer compared to that in the bulk (Figure 2b).

Results summarized in Figure 3 show that the F:C ratios increase while the O:C ratios decrease with an increase of the fluorine bulk concentration from %F = 0 wt % to %F = 6.24 wt %. At higher fluorine contents (%F > 6.24 wt %) these ratios remain constant. Evidently, the preparation of the films from the melt leads to a higher enrichment of the R_f perfluorinated tails in the topmost layer in comparison to the spin-coated films prepared from the same oligoesters. These results are in very good agreement with the results obtained from contact angle measurements. Note, an increase in the water and *n*-hexadecane contact angles was observed while F:C ratios increase and O:C ratios decrease (Figures 1 and 3). Moreover, higher advancing water and *n*-hexadecane contact angles at higher F:C ratios were

Table 4. Surface (Obtained from ARXPS) and Bulk Elemental Composition as Well as Enrichment Factor (*Q*) of the Spin-Coated and Melt Oligoester Films[a]

				spin-coated films[b]			melt films[b]		
sample ID	F (%)	information depth, (nm)	[F]:[C] in the bulk	[F]:[C]	Q	[O]:[C]	[F]:[C]	Q	[O]:[C]
LO-F8#1	0	8	0	0	0	0.26	0	0	0.19
		4		0	0	0.26	0	0	0.19
		2		0	0	0.27	0	0	0.19
LO-F8#2	2.54	8	0.027	0.32	11.9	0.20	0.35	13.0	0.19
		4		0.35	13.0	0.19	0.51	18.9	0.18
		2		0.42	15.6	0.17	0.61	22.6	0.15
LO-F8#4	6.24	8	0.068	0.37	5.4	0.19	0.40	5.9	0.19
		4		0.54	7.9	0.17	0.58	8.5	0.16
		2		0.61	9.0	0.13	0.65	10.7	0.13
LO-F8#5	10.72	8	0.120	0.39	3.3	0.19	0.41	3.4	0.19
		4		0.56	4.7	0.15	0.56	4.7	0.16
		2		0.65	5.4	0.14	0.70	5.7	0.14

[a] The ARXPR results are obtained from F 1s and C 1s peak area of XPS spectra at 2, 4, and 8 nm information depths. [b] Surface concentration of atoms

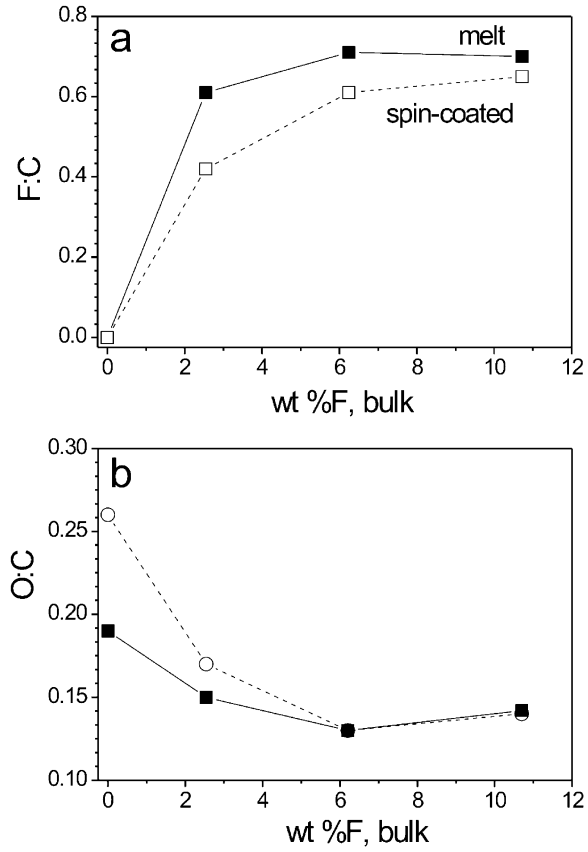

Figure 3. Atomic ratios F:C (a) and O:C (b) at the topmost of spin-coated (open symbols) and melt (solid symbols) polymer film obtained from ARXPS (incidence angle 75°, information depth of 2 nm) vs bulk fluorine contents.

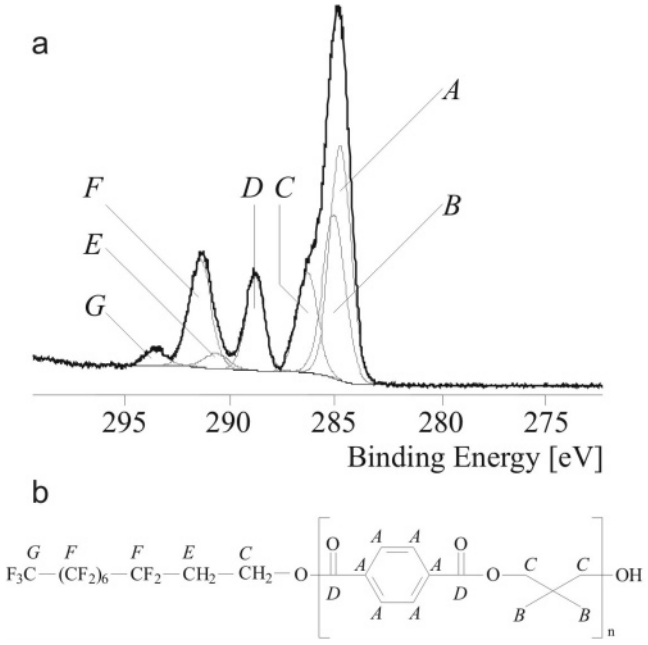

Figure 4. (a) High-resolution C 1s spectrum of the sample LO-F_8#5 recorded at a takeoff angle of 0°. (b) Different carbon species in the polymer chain cause the component peaks *A*, *B*, *C*, *D*, *E*, and *F*.

observed for the melt films compared to the spin-coated ones. Furthermore, the fact that surface concentration of fluorine in samples with %F = 6.24 wt % and %F = 10.72 wt % (LO-F8#4 and LO-F8#5) is almost identical and is in a reasonable agreement with constancy of the HD advancing contact angles at %F ≥ 6.24 wt % (Figure 1b). However, the water advancing contact angles are different for the oligoesters with %F = 6.24 and %F = 10.72 wt % (LO-F_8#4 and LO-F_8#5) although the F:C and O:C ratios are nearly identical for these samples.

In the case of the nonfluorinated oligoester, the lower concentration of the oxygen-containing ester groups (Figure 3b) in the melt films results in higher values of the water advancing contact angles (Figure 1a) and hence in a lower solid surface free energy compared to that of the spin-coated films.

Next, we performed an analysis of highly resolved peak of carbon. A typical C 1s high-resolution spectrum for the fluorinated end-functionalized oligoester LO-F_8#5 (%F = 10.72 wt %) is shown in Figures 4 and 5. The shape of the measured C_{1s} spectrum is a composite of the differently bound carbon atoms. The deconvolution of this C_{1s} spectrum allows identifying the different carbon species and their contribution to the sample's surface composition. The component peak *A* represents the carbon atoms, which are involved in the aromatic system of the phenyl ring. Component peak *B* shows the presence of the two methyl groups in the polyester chain. The two component peaks cannot be well resolved due to strong overlapping. The component peaks *C* and *D* show the alcohol side carbons of the ester group ($H_2C-O-C=O$) and the corresponding ester carbons ($H_2C-O-C=O$). The component peak *F* appears from CF_2 groups of the perfluoroalkyl chain, and the component peak *G* shows its CF_3 end group. The unit that couples the perfluoroalkyl chain to the oligoester is indicated by the component peaks *E* (CF_2-CH_2) and the component peak

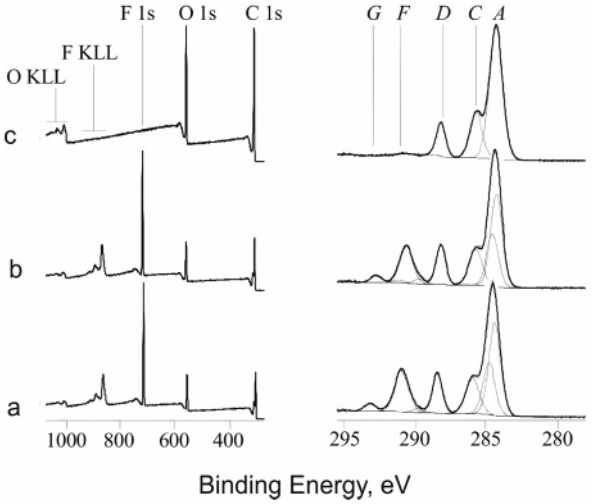

Figure 5. Typical XPS wide-scan and high-resolution C 1s spectra of the spin-coating films recorded at a takeoff angle of 0°: (a) LO-F_8#1, (b) LO-F_8#4, and (c) LO-F_8#5.

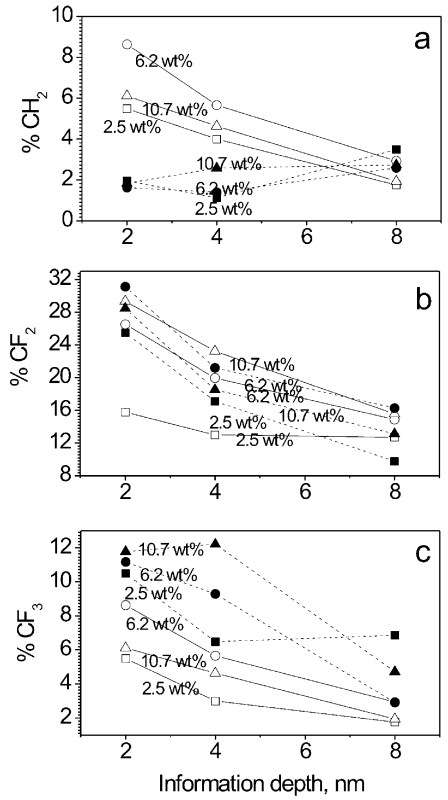

Figure 6. Surface atomic concentration of (a) CH_2, (b) CF_2, and (c) CF_3 groups as a function of the information depth in the melt (solid symbols) and spin-coated films (open symbols) at different bulk fluorine content (▲, △ 10.72 wt %; ●, ○ 6.25 wt %; ■, □ 2.54 wt %).

of the ester group *D*. Concerning the given stoichiometry, the intensities of the two component peaks have to be equal.

The perfluoroalkyl tail is composed of the head CF_3 group, a sequence of seven CF_2 groups, and two methylene groups coupling the perfluoroalkyl rests and the oligoester. The depth-resolved concentration profile of these groups and the intensity ratios between them can provide the information about conformation and packing of the perfluorinated tails. The results presented in Figure 5 imply that the migration of an additional amount of CF_3 groups to the surface occurs in the melt film replacing the CH_2 groups, which move into the bulk phase. The

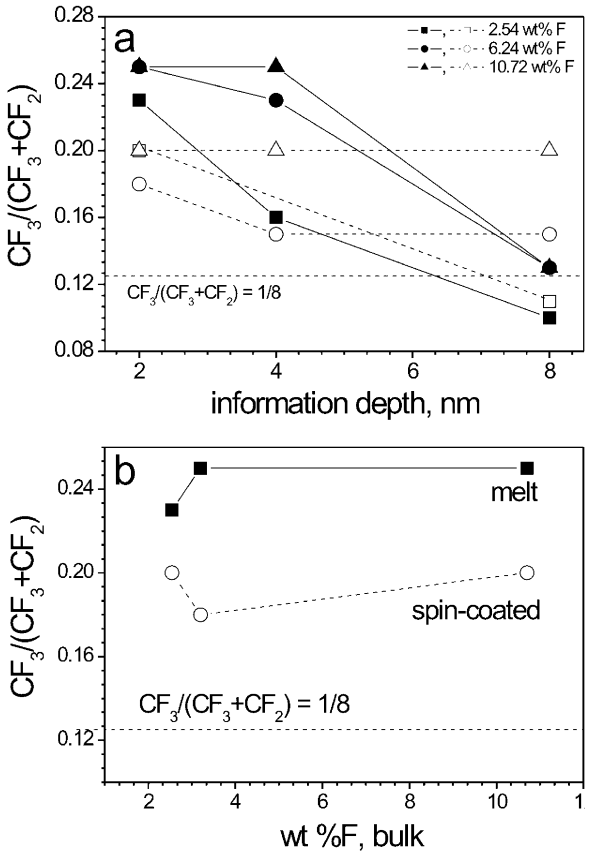

Figure 7. Relative concentration of the fluorinated species $CF_3/(CF_2 + CF_3)$ as a function of the bulk fluorine content in the melt (solid symbols) and spin-coated films (open symbols) for the upper 2 nm thick layer.

concentration of CF_2 groups is distinctly higher for the melt film of the sample LO-F8# 2 which contains %F = 2.54 wt % of fluorine comparing to the spin-coated one (Figure 6b). The CF_2 group concentration in the surface region is independent of the film preparation conditions for the oligoesters with the higher (%F > 2.54 wt %) bulk fluorine content. Therefore, in the case of lower fluorine content (%F = 2.54 wt %) it can be assumed that there are two processes which determine the surface properties of the oligoester films. These may be stronger migration and better alignment of perfluorinated tails if the oligoester surface is not saturated with fluorine groups. A higher degree of fluorination in the bulk leads to a saturation of the surface, and annealing in melts predominantly leads to a higher surface enrichment and closer packing of perfluorinated species.

It was found that ratio $CF_3/(CF_3 + CF_2)$, which was calculated from the high-resolution C_{1s} spectra, decreases with an increase of the information depth (Figure 7a). Apparently, this decrease is more pronounced for the melt layers. The value of $CF_3/(CF_3 + CF_2)$ for the uppermost 2 nm information depth is almost independent of the bulk fluorine contents and slightly higher for the melt films comparing to the spin-coated ones. It can be assumed that for a homogeneous distribution of the perfluorinated tails the value of $CF_3/(CF_3 + CF_2)$ should coincide with the value of the stoichiometric ratio $CF_3/(CF_3 + CF_2)$ in the fluorine tail $(CF_3/(CF_2 + CF_3)_{tail} = 1/8)$. Thus, any deviations from the stoichiometry indicate some preference of perfluorinated tails to the surface and better ordering. The sensitivity of XPS fades out with the depth where the photoelectrons are produced so that atoms located deeper (CF_2 groups) give less intensity than atoms located closer to the surface (CF_3 groups). Therefore, the high experimental value of $CF_3/(CF_3 + CF_2)$

indicates stretching of perfluorinated tails so that higher content of CF_3 groups are on the top surface. We assume that a more densely packed R_f end chains with closer arrangement of CF_3 groups on the top of the surface in melt films. In the spin-coated films, the degree of surface arrangement of perfluoroalkyl substitutes is smaller (Figure 7b). This difference between the enrichment of R_f groups in the outermost surface region of melt and spin-coated layers was found to be in a good correlation with the wetting properties.

Conclusions

In summary, we have reported a thorough investigation of the effect of processes of the fluorine surface segregation in correlation with the wettability on the surface properties of perfluoroalkyl end-functionalized linear aromatic oligoesters. We have shown that perfluoroalkyl end-functionalized linear aromatic oligoesters are very promising systems to design coatings with extreme low water and oil repellency.

For the first time we described an influence of the method of film preparation from fluorinated polymers onto their surface properties. We have compared properties of films containing different fluorine concentration prepared by the spin-coating technique and following annealing and by melting of polymer grain onto the supported substrate.

We demonstrated that both methods can be successfully used for the preparation of highly hydrophobic and oleophobic surfaces. Moreover, oligoester films with the surface energies as low as 11 mJ/m^2 were prepared with 10.72 wt % of fluorine in the system. It is noteworthy that these values are lower than those of commercially available fluorinated polymers, such as Teflon AF. Whereas the water repellence of the perfluorinated oligoesters is smaller due to higher contact angle hysteresis compared to Teflon AF, they possess a higher oleophobicity. However, the advantage of the use of the melting of polymer grain for the preparation of polymer layer is that it allows to achieve a higher surface enrichment and closer packing of perfluorinated species and as a result a higher hydro/oleophobicity, especially at lower F contents (<6 wt %). Moreover, in the present study, the surface hydrophobicity and oleophobicity were deeply analyzed and discussed in terms of contact angle hysteresis and not only advancing contact angle.

The enrichment of the outermost surface region with the perfluoroalkyl substitutions was proved by angle-resolved ARXPS. ARXPS results showed a stronger surface segregation of the perfluorinated terminating groups for the melts. This result was found to be in good correlation with the contact angle data.

We foresee a large potential of investigated systems based on the thick melt films in real coating applications. In addition, we believe that our study can give qualitatively and quantitatively new knowledge about the surface properties of perfluorinated linear aromatic oligoesters for prediction/control of the wetting behavior and adhesion.

Acknowledgment. We thank Leonid Ionov for helpful comments on the manuscript. This work was supported by the German Ministry of Education and Research (BMBF) (Project No. 01 RC 0040). Authors thank Dieter Pleul for XPS measurements.

References and Notes

(1) Pittman, A. G. In *Fluoropolymers*; Wall, L. A., Ed.; Wiley: New York, 1972; Vol. 25, p 419.
(2) Coelho, M. A. N.; Vieira, E. P.; Motschmann, H.; Mohwald, H.; Thunemann, A. F. *Langmuir* **2003**, *19*, 7544−7550.
(3) Lee, W.-K.; Toselli, M.; Gardella, J. A. *Macromolecules* **2001**, *34*, 3493−3496.
(4) Davies, M. C.; Shakesheff, K. M.; Shard, A. G.; Domb, A.; Roberts, C. J.; Tendler, S. J. B.; Williams, P. M. *Macromolecules* **1996**, *29*, 2205−2212.
(5) Grundke, K.; Zschoche, S.; Poschel, K.; Gietzelt, T.; Michel, S.; Friedel, P.; Jehnichen, D.; Neumann, A. W. *Macromolecules* **2001**, *34*, 6768−6775.
(6) Grundke, K.; Pospiech, D.; Kollig, W.; Simon, F.; Janke, A. *J. Colloid Polym. Sci.* **2001**, *279*, 727.
(7) Appelhans, D.; Wang, Z.-G.; Zschoche, S.; Zhuang, R.-C.; Haussler, L.; Friedel, P.; Simon, F.; Jehnichen, D.; Grundke, K.; Eichhorn, K.-J.; Komber, H.; Voit, B. *Macromolecules* **2005**, *38*, 1655−1664.
(8) Yang, S.; Wang, J.; Ogino, K.; Valiyaveettil, S.; Ober, C. K. *Chem. Mater.* **2000**, *12*, 33−40.
(9) Feng, L.; Song, Y.; Zhai, J.; Liu, B.; Xu, J.; Jiang, L.; Zhu, D. *Angew. Chem.* **2003**, *115*, 824−826.
(10) Woodward, I.; Schofield, W. C. E.; Roucoules, V.; Badya, J. P. S. *Langmuir* **2003**, *19*, 3432−3438.
(11) Vargo, T. G.; Thompson, M.-F.; Gerenser, L. J.; Valentini, R. F.; Aebischer, P.; Hook, D. J.; Gardella, J. A. *Langmuir* **1992**, *8*, 130−134.
(12) Lenk, T. J.; Hallmark, V. M.; Hoffmann, C. L.; Rabolt, J. F. *Langmuir* **1994**, *10*, 4610−4617.
(13) DeSimone, J. M.; Guan, Z.; Elsbernd, C. S. *Science* **1992**, *257*, 945.
(14) Thomas, R. R.; Anton, D. R.; Graham, W. F.; Darmon, M. J.; Stika, K. M. *Macromolecules* **1998**, *31*, 4595−4604.
(15) Krupers, M.; Slangen, P.-J.; Moller, M. *Macromolecules* **1998**, *31*, 2552−2558.
(16) O'Rourke Muisener, P. A. V.; Jalbert, C. A.; Yuan, C.; Baetzold, J.; Mason, R.; Wong, D.; Kim, Y. J.; Koberstein, J. T.; Gunesin, B. *Macromolecules* **2003**, *36*, 2956−2966.
(17) O'Rourke-Muisener, P. A.; Koberstein, J. T.; Kumar, S. *Macromolecules* **2003**, *36*, 771−781.
(18) Koberstein, J. T. *J. Polym. Sci., Part B* **2004**, *42*, 2942.
(19) Hunt, M. O.; Belu, J. A. M.; Linton, R. W.; DeSimone, J. M. *Macromolecules* **1993**, *26*, 4854−4859.
(20) Ming, W.; Lou, X.; van de Grampel, R. D.; van Dongen, J. L.; van der Linde, R. *Macromolecules* **2001**, *34*, 2389−2393.
(21) Ming, W.; Tian, M.; van de Grampel, R. D.; Melis, F.; Jia, X.; Loos, J.; van der Linde, R. *Macromolecules* **2002**, *35*, 6920−6929.
(22) van de Grampel, R. D.; Ming, W.; Gildenpfennig, A.; Laven, J.; Brongersma, H. H.; de With, G.; van der Linde, R. *Langmuir* **2004**, *20*, 145−149.
(23) van de Grampel, R. D.; Ming, W.; Gildenpfennig, A.; van Gennip, W. J. H.; Laven, J.; Niemantsverdriet, J. W.; Brongersma, H. H.; de With, G.; van der Linde, R. *Langmuir* **2004**, *20*, 6344−6351.
(24) Hirao, A.; Koide, G.; Sugiyama, K. *Macromolecules* **2002**, *35*, 7642−7651.
(25) Chen, Z.; Ward, R.; Tian, Y.; Baldelli, S.; Opdahl, A.; Shen, Y.-R.; Somorjai, G. A. *J. Am. Chem. Soc.* **2000**, *122*, 10615−10620.
(26) Affrossman, S.; Bertrand, P.; Hartshorne, M.; Kiff, T.; Leonard, D.; Pethrick, R. A.; Richards, R. W. *Macromolecules* **1996**, *29*, 5432−5437.
(27) Baetzold, J. P.; Koberstein, J. T. *Macromolecules* **2001**, *34*, 8986−8994.
(28) Wenzel, R. N. *Ind. Eng. Chem. Res.* **1936**, *28*, 988.
(29) Kwok, D. Y.; Neumann, A. W. *Adv. Colloid Interface Sci.* **1999**, *81*, 167.
(30) Kwok, D. Y.; Gietzelt, T.; Grundke, K.; Jacobasch, H.-J.; Neumann, A. W. *Langmuir* **1997**, *13*, 2880−2894.
(31) Kwok, D. Y.; Neumann, A. W. *Adv Colloid Interface* **1999**, *81*, 167−249.
(32) Grundke, K. In *Molecular Interfacial Phenomena of Polymers and Bipolymers*; Chen, P., Ed.; Woodhead Publishing: Cambridge, UK, 2005; Vol. 10, pp 323−374.
(33) For convenience, we will denote water advancing/receding contact angles as Θ_A^W/Θ_R^W and *n*-hexadecane advancing/receding contact angles as $\Theta_A^{HD}/\Theta_{R^D}$, respectively.
(34) Wu, S. *Polymer Interface and Adhesion*; Marcel Dekker: New York, 1982.
(35) Grundke, K. In *Phenomena in Surface Chemistry*; Holmberg, K., Ed.; John Wiley & Sons: New York, 2001; pp 119−142.
(36) Tavana, H.; Yang, G.; Yip, C. M.; Appelhans, D.; Zschoche, S.; Grundke, K.; Hair, M. L.; Neumann, A. W. *Langmuir* **2006**, *22*, 628−636.
(37) Tavana, H.; Petong, N.; Hennig, A.; Grundke, K.; Neumann, A. W. *J. Adhes.* **2005**, *81*, 29−39.
(38) Seah, M. P. In *Practical Surface Analysis by Auger and X-ray Photoelectron Spectroscopy*; Briggs, D., Seah, M. P., Eds.; Wiley: Chinchester, 1990; pp 202−255.
(39) Shirley, D. A. *Phys. Rev.* **1972**, *B5*, 58.

(40) Van de Grampel, R. D.; Ming, W.; Laven, J.; van der Linde, R.; Leermakers, F. A. M. *Macromolecules* **2002**, *35*, 5670−5680.
(41) vanRavenstein, L.; Ming, W.; van de Grampel, R. D.; van der Linde, R.; de With, G.; Loontjens, T.; Thune, P. C.; Niemantsverdriet, J. W. *Macromolecules* **2004**, *37*, 408−413.
(42) Sauer, B. B.; McLean, R. S.; Thomas, R. R. *Langmuir* **1998**, *14*, 3045−3051.
(43) Adamson, A. W. In *Physical Chemistry of Surfaces*, 5th ed.; Wiley: New York, 1990; p 368.
(44) Chen, W.; Fadeev, A. Y.; Hsieh, M. C.; Oner, D.; Youngblood, J.; McCarthy, T. J. *Langmuir* **1999**, *15*, 3395−3399.

MA061139I